JOURNAL OF MATERIALS SCIENCE 32 (1997) 5545–5550

Laser beam processing of a SiC particulate reinforced 6061 aluminium metal matrix composite

LI HONG, R. M. VILAR
Laser Laboratory, Departamento de Engenharia de Materiais, Institute Superior Tecnico, Av. Rovisco Pais, 1096 Lisbon Codex, Portugal

WANG YOUMING
Department of Metal Forming , University of Science and Technology Beijing, Beijing 100083, Peoples Republic of China

SiC particulate reinforced 6061 Al metal matrix composites were laser beam cut using a 3kW continuous wave CO_2 laser. The influence of laser processing parameters such as cutting speed, laser power, and shielding gas on the quality of the cuts were investigated. Optical microscopy, scanning electron microscopy and X-ray diffraction were used to analyse the laser treated zone. Experimental results show that 6061 Al metal matrix composites can be cut successfully using a laser. A number of Al_4C_3/Al_4SiC_4 plates were formed in the heat affected zones due to a chemical reaction between Si and Al that occurred during the laser processing.

1. Introduction

SiC/Al_2O_3 particulate reinforced Al metal matrix composites (MMCs) are extensively used in the aerospace, automobile and sports industries due to their high strength, light weight, low coefficient of thermal expansion, good thermal conductivity and excellent wear and abrasion resistance compared to their monolithic counterparts [1]. In many of these applications it is desirable to fabricate the metal matrix composites into complex shapes. Unfortunately, most current methods for manufacturing MMCs, i.e., powder processing, extrusion, squeeze casting and hot isostatic pressing, are limited to simple shapes. Most simple shaped components are subsequently trimmed to net size and attached to an assembly by adhesive bonding. Due to the presence of both hard and soft phases in the composites, the cutting or welding of MMCs is difficult.

Laser beam machining of MMCs is fast replacing most other conventional methods. The ability of the laser to cut intricate shapes and complex patterns and weld either similar or dissimilar materials with minimum distortion and a negligible heat affected zone (HAZ) make it a highly competitive manufacturing method [2]. Aluminium based alloys and composite materials are characterized by a low absorption factor for a CO_2 laser beam and a high thermal conductivity [3]. The resultant low viscosity of the liquid melt makes laser processing difficult. Despite these drawbacks, several papers in the literature have reported on the laser machining and welding of Al metal matrix composites. Lau *et al.* [4] have investigated the laser cutting behaviour of a SiC/Al–Li MMC (20% wet SiC_p + 8090Al). Kudapa *et al.* [2] have reported successfully laser cutting and welding 10 vol% Al_2O_3 particulate reinforced 6061 Al and 15 vol% SiC whisker reinforced 2009 Al whilst Kawali and Viegelahn [5] have laser welded 20 vol% Al_2O_{3p} reinforced 6061 Al. Dahotre and his colleagues [6–8] have performed an extensive investigation on the laser welding of 10–20 vol% SiC_p reinforced A356 Al. In particular a detailed analysis was performed on the microstructures of the melting zone and the heat affected zone. A chemical reaction between SiC and aluminium was observed to occur during the laser processing in their study. However, all the previously reported work focused on the low volume fraction content reinforced phases (< 20 vol%). The purpose of the present work is to evaluate the possibility of laser cutting high SiC volume per cent content 6061 Al MMC (60 vol%SiC) and characterize the microstructure of the cutting surface and HAZ.

2. Experimental procedure

The material used in this study is 60 vol % SiC and a 6061 Al MMC produced by squeeze casting. The average SiC particle size is 7 μm. The casting plate with a thickness of 10 mm was isothermally rolled at a temperature of 550°C. The rolling was carried out using a reduction of 0.5 mm per pass until a final thickness of about 1.5 mm was reached. The laser processing was performed on this rolled MMC sheet. A 3 kW power continuous wave CO_2 laser was used at an operating power of 2.5 kW in all the experiments. The laser beam was focused 0.5 mm below the MMC sheet surface. The cutting speed was controlled by a precision *x*-*y* table. Three cutting speeds of 15, 25

0022–2461

and 35 mm s^{-1} were applied. Argon gas was used to prevent oxidation and blow away debris. Because of the presence of a high SiC content in the material, which enhanced the laser beam coupling, no surface modification was made before the cutting was performed. Microstructural observation of the as-cut surface and cross-sections of the as-cut surface were performed using an Olympus optical microscope and a Hitachi S-2400 scanning electron microscope (SEM). When polishing the cross-section of an altered surface, special techniques for mounting and polishing were used to reduce edge rounding. In this investigation, the samples were first cut by a diamond saw and were then mounted in Bakelite with a backup plate to ensure edge retention, during the polishing. In order to identify the phases within the laser treated zone, X-ray diffraction was performed on cut surface using a Cu$K_{\alpha 1}$ radiation.

3. Results

The optical micrographs of the isothermal rolled 60 vol% SiC/6061 Al MMC are shown in Fig. 1(a and b). As can be observed in the photographs, the microstructure consists of SiC particulates (sized between 3.5–10 μm) and small Mg_2Si particles of size 0.1 μm in an Al matrix. It is noted that some of the SiC particulates were broken during rolling.

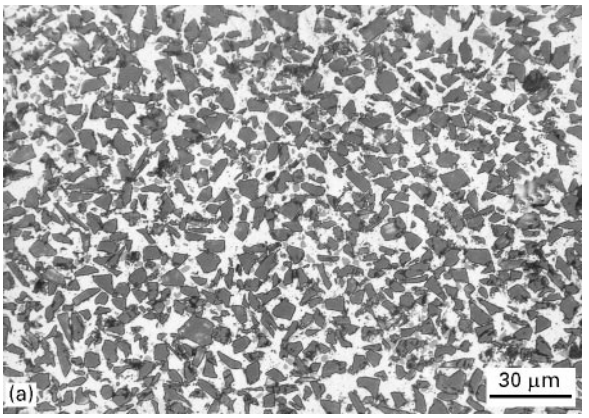

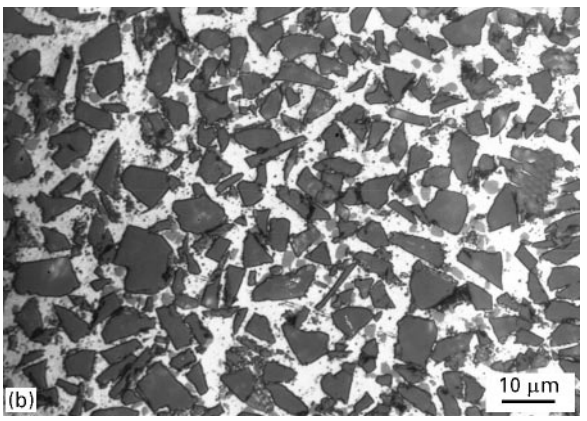

Figure 1 The optical micrographs of isothermal rolled 60 vol% SiC/6061 Al MMC. (a) The microstructure consists of SiC particulates uniformly distributed in an Al matrix. (b) At high magnification small Mg_2Si particles are visible.

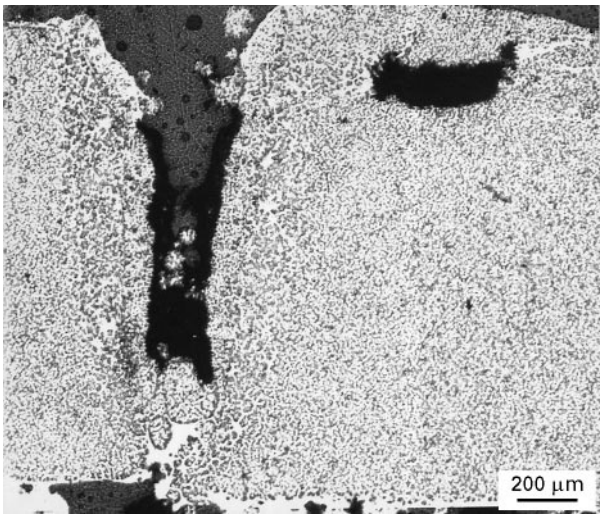

Figure 2 Cross-sectional micrograph of the laser cut surface at $v = 25$ mm s^{-1} and $p = 2.5$ kW.

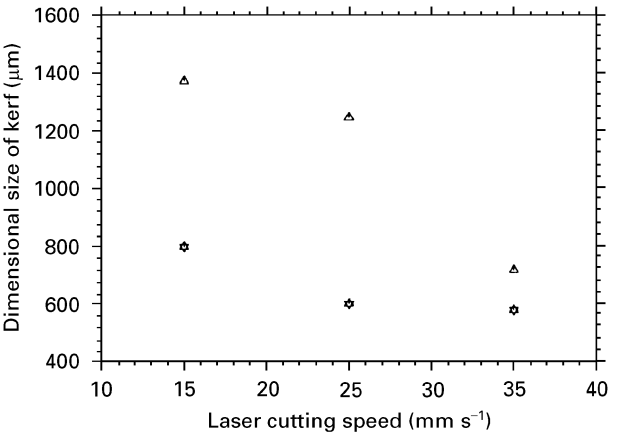

Figure 3 The depedence of (△) the depth and (☆) the width of cutting kerf on cutting speed.

Fig. 2 is the cross-sectional view of the surface laser cut at 25 mm s^{-1} and 2.5 kW. The morphology of the kerf is typical for high energy laser processing. The cutting speed as a function of depth and width of the kerf at a power of 2.5 kW is shown in Fig. 3. The depth and width of the cutting kerf decrease with an increase in the cutting speed, this result is in agreement with that of Kudapa *et al.* for the laser cutting of 10 vol% Al_2O_{3p} reinforced 6061 Al [2]. The reason for this is that at a given power level, higher speeds mean that a lower amount of energy is available to remove material in the cut zone.

SEM micrographs of the microstructure of the as-cut surface are shown in Fig. 4(a–f). At a high cutting speed of 35 mm s^{-1} the surface is very rough and straddled with striations (Fig. 4a). For most beam processing methods, this is a common observation for the cut surface. The striations on the cutting surfaces were due to the unsteady motion of the molten layer or melt flow oscillation. Intermittent plasma blockage can also play a part in the formation of surface striations [3]. A low cutting speed of 15 mm s^{-1} produced a relatively smooth surface (Fig. 4b) as compared to a high cutting speed. High magnification micrographs

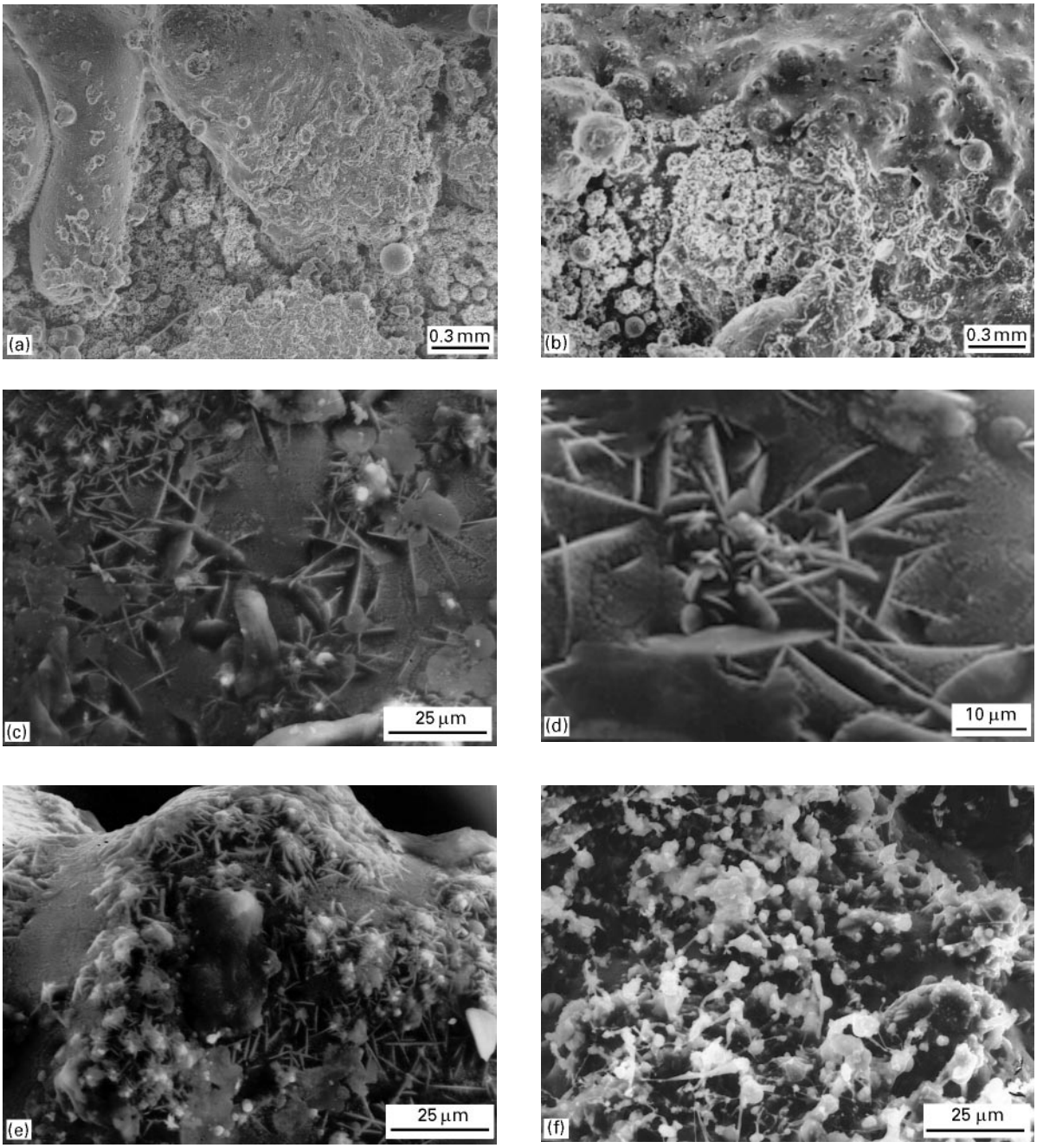

Figure 4 The SEM microstructures of laser cut SiC/6061 Al MMC surface. (a) Cut at 15 mm s^{-1}, the surface is rough; (b) cut at 35 mm s^{-1} the surface is relatively smooth; (c), (d) and (e) high magnification structures cut at 15, 25 and 35 mm s^{-1}, respectively, some Al_4C_3 plates are observed; and (f) structure at the bottom of kerf cut at 25 mm s^{-1}.

of the microstructures produced at cutting speeds of 35, 25 and 15 mm s^{-1} are shown in Fig. 4 (c–e) respectively. It is interesting to observe that the laser cut surfaces are characterized by white plate/needle-like phases. Near the top of the kerf the size of the plate-like phase is small (3–5 μm in length). In most of the other areas the length of the plates is between 10–20 μm. Some polygonal particles were found to have precipitated onto the white needle phase (Fig. 4d). The grain size of the Al matrix is significantly refined (5–10 μm) by the rapid solidification produced by the laser beam (Fig. 4(d and e)). However, at the bottom of the kerf (laser cut at a speed of 25 mm s^{-1}) white spheroidal particles are observed to predominate instead of the plate/needle-like phases (Fig. 4f).

Fig. 5 displays the X-ray diffraction pattern obtained from the surface cut at a speed of 25 mm s^{-1}. The reflections could be indexed in terms of the carbides Al_4C_3, Al_4SiC_4, and SiC and elemental Al and Si.

The cross-sectional microstructures after laser cutting at a speed of 25 mm s^{-1} are illustrated in Fig. 6(a–f). It can be seen from Fig. 6 (a–c) that four distinct regions were produced in the composite after laser cutting. An overheated region A is observed close to the cutting surface with a narrow width of 50–60 μm (Fig. 6a). This area contains very fine plate/needle-like phases, small SiC particles and some blocky Si particles distributed in an Al matrix (Fig. 6(b and d)). Region B is next to region A and its width is about 200 μm (Fig. 6a). This region is

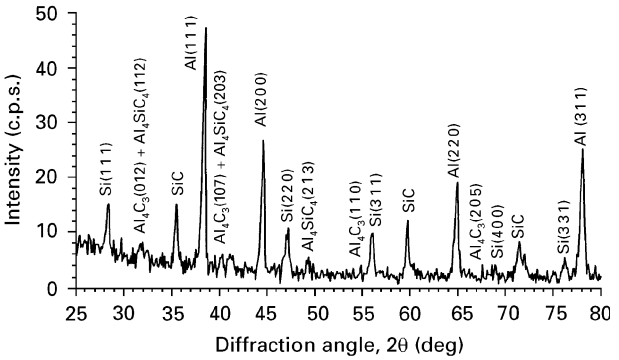

Figure 5 The X-ray diffraction pattern for the laser cutting surface ($v = 25$ mm s^{-1}).

characterized by the redistribution of SiC (Fig. 6(b and e)). The SiC particles show some degree of surface modification and their edges have been smoothed. Furthermore, the particle size of the SiC is clearly increased to between 10–15 μm. Some large blocky Si, fine cellular/dendritic Al structures and Al/Si eutectics are apparent in this region (Fig. 6e). Region B is followed by the partially melted transition zone (region C) which is about 70 μm in width (Fig. 6a). This area consists of plate/needle-like phases between 8–10 μm in size and SiC particles (Fig. 6(c and f)). The plates/needles are nucleated at the surface of the SiC (Fig. 6f). Region D is the unmelted base materials.

The high magnification microstructure shown in Fig. 7 is taken from the area between regions A and B. The morphology of the needle-like phases in this

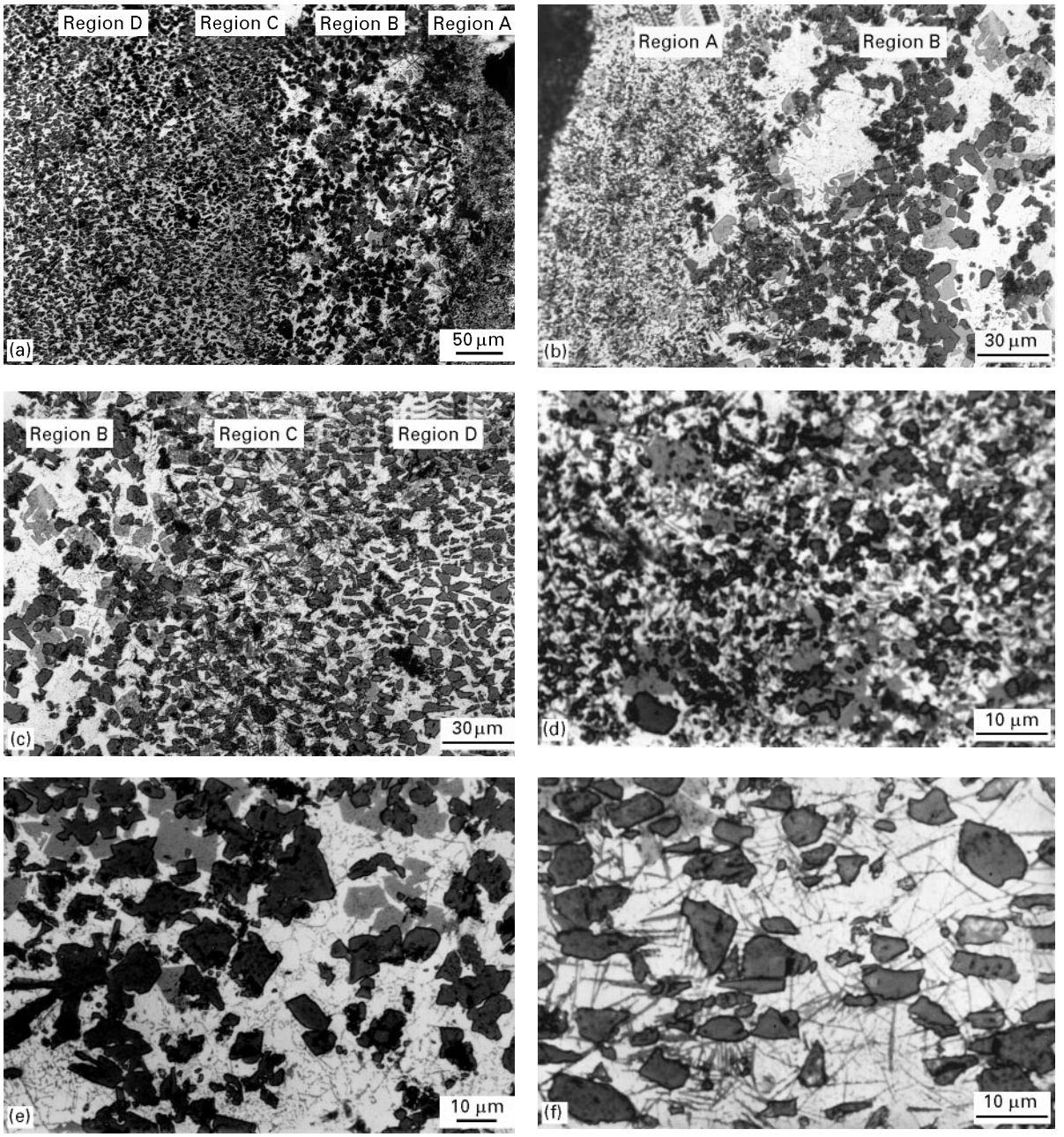

Figure 6 The cross-sectional microstructures after laser cutting at $v = 25$ mm s^{-1}. (a) Low magnification structure containing regions A, B, C, and D; (b) regions A and B; (c) regions B and C; (d) high magnification structures of region A, this area contains very fine plate/needle-like Al_4C_3 plates, small SiC particles and some blocky Si particles distributed in an Al matrix; (e) region B, some large blocky Si (grey) and SiC (black), fine cellular/dendritic Al structure and Al/Si eutectics are apparent; and (f) region C, Al_4C_3 plates are nucleated at the surface of SiC.

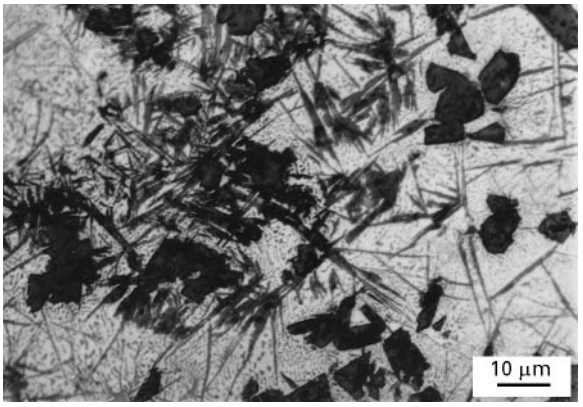

Figure 7 The microstructure in the area between region A and region B. The complex plate/needle-like phases are probably Al_4SiC_4.

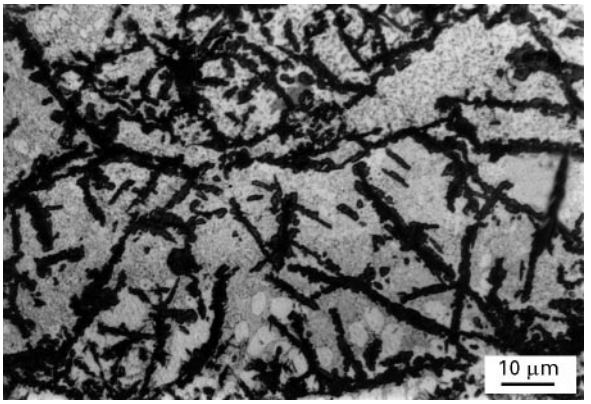

Figure 8 Optical structure in the bottom of the kerf. Some SiC alignments were observed in an Al/Si eutectic matrix.

region is different from those observed in regions A and C. The plates present a complex shape and a large dimension with some plates being probably nucleated inside the SiC particulates. At the bottom of the kerf some strings formed by small SiC particles were found in the matrix of Al and Al/Si eutectics (Fig. 8).

4. Discussion

It is well known that, during the processing of bulk composites, SiC reacts with liquids to form Al_4C_3/Al_4SiC_4 and free silicon. Based upon the interfacial studies by Iseki *et al.* [10] and Viala *et al.* [9], the Al_4C_3/Al_4SiC_4 were probably formed by the reactions:

$$4Al + 3SiC \rightarrow Al_4C_3 + 3Si \quad (1)$$

$$4Al + 4SiC \rightarrow Al_4SiC_4 + 3Si \quad (2)$$

Viala *et al.* [9] have shown that metastable equilibria exist when heating mixtures of SiC and Al below 2000°C. Between 650–1347°C, Al_4C_3 is the reaction product whilst in the temperature range of 1347–1627°C, the reaction produces both Al_4SiC_4 and Al_4C_3. Other related works on laser surface melting and laser cladding of SiC/Al MMCs have shown that the Al_4C_3/Al_4SiC_4 plates were formed due to the reaction between SiC and Al [11–16].

In the laser cutting processing, the intense heat developed by the laser melts the SiC and provides free C for reaction with Al. In region A (close to the cutting surface), the plate/needle-like phases (Fig. 4 (c–e) and Fig. 6(a–c) produced by the chemical reaction between SiC and Al are identified as Al_4C_3 (Fig. 5). The existence of Al_4C_3 is at the expense of SiC. The Al_4C_3 plate is usually thin and is nucleated at the surface of the SiC. The formation of Al_4C_3 is proceeded by a dissolution-recrystallization mechanism [9]. The polygonal phases which precipitated on the Al_4C_3 needles (Fig. 4c) are Si, this observation is in agreement with the results of Dahotre and co-workers [6–8] in their studies on the SiC/A356 Al MMC structure in the laser welding zone. In terms of size and morphology, the plate-like phase in Fig. 7 is large and complex and is probably Al_4SiC_4. The X-ray diffraction pattern displayed in Fig. 5 indicates the existence of this ternary carbide. The microstructure in Fig. 7 is quite similar to the Al_4SiC_4 structure developed during the laser coating of Al–Si with SiC observed by Liechti and Blank [11]. The work of Viala *et al.* [9] has shown that the Al_4SiC_4 mainly appears in the form of large platelets and that its formation occurs via nucleation inside the SiC which suggests that the growth of the Al_4SiC_4 may proceed by solid state diffusion. The Al MMC in this study contains a high volume fraction of SiC (60 vol%), which produces a high melting temperature since the SiC absorbs the infrared laser light very efficiently. Since both Al_4SiC_4 and Al_4C_3 are found in region A, the melt temperature in this area is over 1347°C. Although a high melting temperature is reached during the laser processing, the SiC particles still did not completely melt into a liquid. So there are still quite a number of unmelted small 1–2 μm sized SiC particles existing in region A (Fig. 6d). Due to stirring of the melt produced by the laser beam, some small SiC particles fall down to the bottom of the kerf to form SiC alignments (Fig. 8). The white spheroidal particles (Fig. 4f) are unmelted SiC and atomized Al powders.

In region B the size of the SiC particulates becomes large. This phenomenon is important. In terms of the melting temperature, region B is lower than region A, which means that the unmelted SiC particulates in region B have a large size. However, the Al matrix is completely melted in this area and thus the SiC particulates may flow in the Al liquid. Consequently, agglomeration of the SiC particles may occur. During the subsequent solidification, the growth of cellular/dendritic Al will push the SiC particles together into the intercellular or interdendritic areas. The above two factors account for the redistribution and particular size increase of the SiC. In this region some blocky Si particles were observed. Part of the Si particles are from the melted SiC in region B, with the others probably coming from region A. Due to the overheating produced by the laser beam, the boiling material may generate a vapour pressure around the keyhole [4]. When material in region A is vaporized, an over-pressure develops near the keyhole which causes the migration of some Si/SiC particles from region A to region B. The increase in Si content

in region B thought to be the consequence of the redistribution of Si/SiC. There are no obvious Al_4C_3/Al_4SiC_4 needles in region B due to a high Si content. This phenomenon can be explained by recourse to the work of Lloyd [17] on the reaction rate of Si–Al in which whilst the formation of aluminium carbide was initially high, the reaction rate later dropped off to a steady level. This study also showed that a high Si level (> 8 vol%) in the matrix can prevent the formation of Al_4C_3.

In region C both the SiC and aluminium matrix are partially melted due to a low melting temperature, which means that the Si level in the melt is relatively low. Thus Al_4C_3 plates were predominantly found in this transition zone. The Al_4C_3 plates are obviously initiated at the surface of the SiC (Fig. 6f). The melting temperature in this area is approximately between 650–1347°C.

5. Conclusions

The high volume SiC content 6061 Al MMC can be successfully laser cut to achieve a smooth cutting surface and a narrow heat affected zone (HAZ) at a power of 2.5 kW and cutting speeds between 15–35 mm s^{-1} with an argon shielding gas. Plate/needle-like Al_4C_3 and Al_4SiC_4 were formed at the cutting surface due to a chemical reaction occurring between SiC and the aluminium matrix. Three distinct regions were observed in a cross-sectional view of the HAZ. Near the cutting surface the structure is characterized by small Si/SiC particulates, and Al_4C_3/Al_4SiC_4 plates. In the middle of the HAZ the SiC/Si size increased, the redistribution of SiC particles occurred and Al_4C_3 needles did not form due to the high Si content. Close to the base material large Al_4C_3 plates are predominant.

Acknowledgements

The authors are indebted to Dr. N. Braz of the Laser Laboratory at the Institute Superior Tecnico for laser processing the MMCs samples, and to Dr. N. Xiaomin of the Department of Metallurgy and Engineering Materials, Strathclyde University for discussions about the polishing of the MMC samples.

References

1. J. E. ALLISON and G. S. COLE, *JOM*, **45** (1993) 19.
2. S. KUDAPA, V. BARNEKOV and K. MUKHERJEE, in "Laser materials processing IV", edited by J. Mazumder, K. Mukherjee and B. L. Mordike, TMS Annual Meeting (The Minerals, Metals and Materials Society, Warrendale, 1994) p. 223.
3. J. MAZUMDER, in Proceedings of Interdisciplinary Issues in Materials Processing and Manufacturing, vol. 2 edited by S. K. Samanta, R. Komandari, R. McMeaking, M. M. Chen and A. Tseng ASME Annual Meeting, Boston MA 1987 (ASME, New York, 1987) p. 599.
4. W. S. LAU, T. M. YUE, C. Y. JIANG and S. Q. WU, in Machining of composite materials, Proc. of the Symposium on Machining Composite Materials, Chicago, IL, Nov 1992 (ASM International, Novelty OH, 1992) p. 29.
5. S. M. KAWALI and G. L. VIEGELAHN, in Proceedings of the Laser Materials Processing Symposium, B-8 November 1991, San Jose, CA, Vol, 74, edited by E. A. Metzbower, E. Beyes and A. Matsunawa (Laser Institute of America, Orlando FL, 1992) p. 156.
6. N. B. DAHOTRE, T. W. MCCAY and M. H. MCCAY, *J. Appl. Phys.* **65** (1989) 5072.
7. N. B. DAHOTRE, T. W. MCCAY, M. H. MCCAY and S. GOPINATHAN, *J. Mater. Res.* **6** (1991) 514.
8. N. B. DAHOTRE, T. W. MCCAY and M. H. MCCAY, in Proceedings of the Laser Materials Processing Symposium, 24–28 October 1993, Orlando FL, edited by P. Denney, I. Miyamoto and B. L. Mordike (Laser Institute of America, Orlando FL, 1994) p. 189.
9. J. C. VIALA, P. FORTIER and J. BOUIX, *J. Mater. Sci.* **25** (1990) 1842.
10. T. ISEKI, T. KAMEDA and T. MARUYAMA, *ibid* **19** (1984) 1692.
11. T. LIECHTI and E. BLANK, in "Surface modification technologies VIII", edited by T. S. Sudarshan and M. Jeandin (The Institute of Materials, London, 1995) p. 420.
12. K. M. JASIM, R. D. RAWLINGS, R. SWEENEY and D. R. F. WEST, *J. Mater. Sci. Lett.* **11** (1992) 414.
13. D. PANTELIS, E. GIANNETAKI, Y. CHRYSSOULAKIS and P. PONTHIAUX, *Plating and Surface Finishing* **81** (1994) 52.
14. K. MARCELLOU, D. PANTELIS, Y. CHRYSSOULAKIS and M. MANOLATOS, *Memoires et Etudes Scientifiques de La Revue de Metallurgie* **89** (1992) 711.
15. H. J. HEGGE, J. BOETJE and J. T. M. DEHOSSON, *J. Mater. Sci.* **25** (1990) 2335.
16. C. HU and T.N. BAKER, *ibid* **30** (1995) 891.
17. D. J. LLOYD, *Compos. Sci. Technol.* **35** (1989) 159.

Received 13 November 1995
and accepted 19 December 1996